Quaternary and Pliocene faulting in the Taos Plateau region, northern New Mexico

Stephen F. Personius and Michael N. Machette

1984, pp. 83-90. https://doi.org/10.56577/FFC-35.83

in:

Rio Grande Rift (Northern New Mexico), Baldridge, W. S.; Dickerson, P. W.; Riecker, R. E.; Zidek, J.; [eds.], New Mexico Geological Society 35th Annual Fall Field Conference Guidebook, 379 p. https://doi.org/10.56577/FFC-35

This page is intentionally left blank to maintain order of facing pages.

QUATERNARY AND PLIOCENE FAULTING IN THE TAOS PLATEAU REGION, NORTHERN NEW MEXICO

STEPHEN F. PERSONIUS and MICHAEL N. MACHETTE
U.S. Geological Survey, Federal Center, Denver, Colorado 80225

INTRODUCTION

The Taos Plateau region of northern New Mexico contains numerous faults that offset sedimentary and volcanic rocks of Pliocene and Quaternary age. This report discusses these known or inferred faults and summarizes the work of Machette and Personius (unpublished mapping 1984). Although previous small-scale maps of the Rio Grande rift (Woodward and others, 1975; Baldridge and others, 1983) showed many of the features described in this report, our work focuses on faults and folds less than 5 m.y. old.

This report discusses some of the prominent faults in the Taos Plateau region and includes data on the amounts of vertical surface offset (fault throw), ages of faulted deposits, recency of fault movement, and morphology of fault scarps. Amounts of offset were determined in two general ways: (1) from direct field measurements of the net vertical offset of surfaces across the fault, and (2) from indirect measurements from 1:24,000-scale topographic maps, aerial photographs, and published data. The direct measurements probably are accurate to within 10% of the actual surface offsets, whereas the indirect measurements usually reflect the range of values that are common along a fault (for example, 5-20 m of surface offset).

Only faults that displace, or are suspected to displace, Pliocene or younger materials are shown in Figure 1. Many more faults may be present in the area. For example, Pliocene or younger faulting probably occurred, but cannot be demonstrated in areas where only Miocene or older rocks arc exposed; most mapped faults in these areas are not shown. In other areas, deposition or erosion may have removed evidence of Pliocene and younger faulting.

Data used to compile Figure 1 are from published and unpublished geologic maps and literature, inspection of aerial photographs, and limited field investigations of Quaternary fault scarps. The geologic-map data are quite variable, ranging from reconnaissance maps at scales of 1:62,500 or smaller to detailed maps at scales of 1:24,000 or larger. Where several sources of data were available, we used the most recent data that focused on late Cenozoic structural and stratigraphic studies of an area.

Our approach of showing only faults for which direct evidence of Pliocene or younger movement exists yields a minimum number of faults. Readers using these data for hazards assessment, regional structural analysis, or other similar studies should be aware that many other Pliocene or younger faults may be, and probably are, present in the Taos Plateau.

GEOLOGIC SETTING

Because the main subject of this report is Pliocene and Quaternary faulting, we deal with the pre-Pliocene geology of the region by briefly discussing the basic structural setting of the Taos Plateau portion of the northern Rio Grande rift. Recent reports on the region include discussions of the general evolution of the Rio Grande rift by Chapin (1979); the guidebook of the Rio Grande rift compiled by Hawley (1978); a study of upper Cenozoic sedimentary and volcanic rocks of the Taos area by Lambert (1966); the geology of the Taos Plateau by Lipman and Mehnert (1979); and the geology of the Espafiola Basin by Manley (1979). The following discussion is a broad overview of the late Cenozoic history of the Rio Grande rift in northern New Mexico.

The area covered in this report includes the northernmost part of the Espairiola Basin, the southeastern edge of the Chama Basin, and the Taos Plateau (the southern part of the San Luis Basin). These basins are separated by two major structural elements: (1) the Brazos uplift, a southeast-trending ridge of Precambrian basement rock (Cordell, 1978) that terminates southward near Cerro Azul, and (2) the northeast-trending Embudo fault that parallels the Rio Grande in the southern part of the map area (Muehlberger, 1979). The Embudo fault is coincident with the Jemez lineament (Lambert, 1966; Cordell, 1978) where it traverses the Rio Grande rift. Outside of the rift, the Jemez lineament is marked by a northeast-trending alignment of late Miocene to Holocene volcanic centers (including the Jemez caldera) that extend from southwestern New Mexico to southeastern Colorado (Lambert, 1966).

The general structural pattern of the Taos Plateau region is that of a half graben with major displacement on the eastern margin of the rift, along the western front of the southern Sangre de Cristo Mountains. Gravity data suggest that this part of the rift is underlain by 5 km or more of basin-filling rocks (L. E. Cordell, unpubl. data cited *in* Lipman and Mehnert, 1979). Taking the topographic relief between the Taos Plateau and the Sangre de Cristo Mountains into account, Precambrian to lower Tertiary rocks may be offset by as much as 7-8 km along the east margin of the rift (Lipman and Mehnert, 1979). Conversely, the western margin of the rift is indistinctly marked by flows of the Servilleta Basalt that lap onto eastward-tilted pre-rift to early-rift volcanic and sedimentary rocks. A north—northwest-trending zone of small displacement, down-to-the-west antithetic normal faults that cut Pliocene Servilleta Basalt, forms the western boundary of the Rio Grande rift in the Taos Plateau region.

The central part of the region is dominated by the Taos Plateau volcanic field (Upson, 1939; Lambert, 1966; Lipman and Mehnert, 1979; Dungan and others, this volume). Tholeiitic lavas of the Pliocene Servilleta Basalt erupted from shield volcanoes, and are the most voluminous and widespread rock type on the plateau. About 150 m of flood basalt is exposed in the Rio Grande gorge, which bisects the southern part of the Taos Plateau. Here as many as 15 basalt flows form three sequences that are interbedded with sediment of the upper part of the Santa Fe Group (Lipman and Mehnert, 1979). Most K—Ar age determinations from flows of the Servilleta Basalt are concentrated in a narrow range from 3.6 to 4.5 m.y. (Ozima and others, 1967; Lipman and Mehnert, 1979). However, dates of 2.8 m.y. (Manley, 1979) and 4.6 m.y. (Baldridge and others, 1980) have been obtained on upper flows of the Servilleta Basalt in the Black Mesa and Rio Grande gorge areas, respectively. Despite these conflicting dates, Dungan and others (this volume) have chosen to use the chronology of Ozima and others (1967) and Lipman and Mehnert (1979) in their detailed examination of the Taos Plateau volcanic field.

The thick sequence of Santa Fe Group sediments within the northern Rio Grande rift provides a stratigraphic record of faulting during Miocene through Pleistocene time. The Tesuque and Chamita Formations of the lower part of the Santa Fe Group (Galusha and Blick, 1971; Manley, 1979) record the depositional response to Miocene uplift and extension; these and coeval units in the southern Rio Grande rift were deposited in a series of closed, fault-bounded basins.

Renewed extension, coupled with regional uplift and a subsequent increase in runoff in the early Pliocene (Chapin, 1979), resulted in establishment of the Rio Grande as a major integrated system that flowed southward through southern Colorado and New Mexico into northern Mexico. During the Pliocene and much of the Pleistocene, the ancestral Rio Grande and its tributary streams deposited a thick sequence of fluvial, bolson, and deltaic sediments in a series of elongate depressions

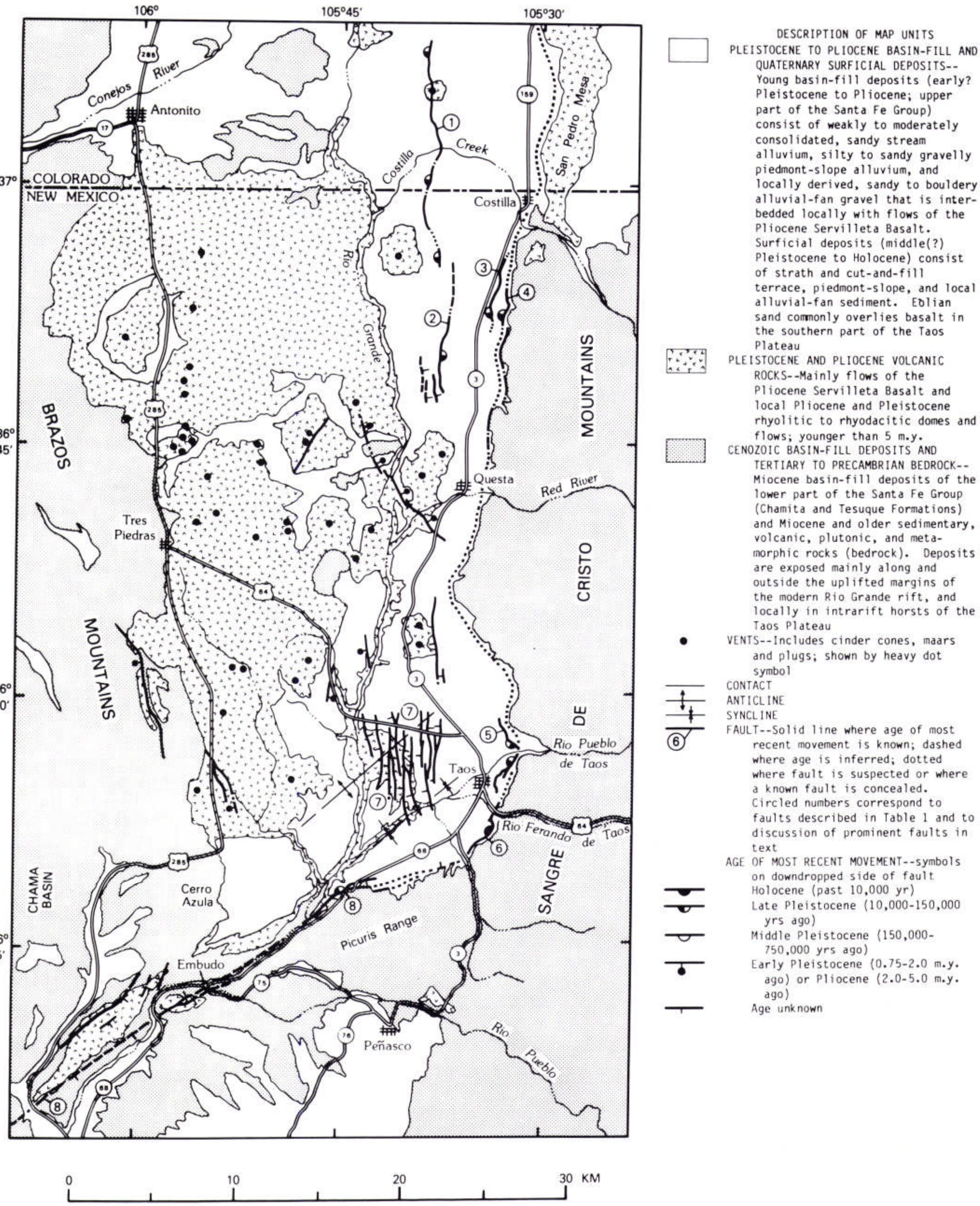

FIGURE 1. Map showing Pliocene and Quaternary faults in the Taos Plateau region, northern New Mexico.

along the length of the Rio Grande rift. These sediments are known collectively as the upper Santa Fe Group. In northern New Mexico the upper part of the Santa Fe Group is represented by the Pliocene Ancha and Puye Formations, and in the remainder of New Mexico it is represented by the Pliocene and Pleistocene Sierra Ladrones and Camp Rice Formations. Tilting of lower Santa Fe Group rocks during or before the early Pliocene created a strong unconformity that commonly separates the two parts of the Santa Fe Group. In the Espanola Basin, the upper part is composed of fanglomerates derived from opposite sides of the rift; the Puye Formation sediments were shed from volcanic highlands in the Jemez Mountains along the west side of the rift, and the Ancha Formation sediments were shed from the Precambrian-cored Sangre de Cristo Mountains east of the rift (Manley, 1979). Alluvium deposited by the Rio Grande in Pliocene time also is included in the upper part of the Santa Fe Group.

Along the upper reach of the ancestral Rio Grande (those parts in New Mexico and Colorado), deposition in the rift basins contained from 4-5 m.y. to perhaps 0.5 m.y. ago, at which time the upper and lower reaches of the Rio Grande were connected at El Paso, Texas. Base level along the upper Rio Grande dropped drastically as a result of this drainage integration. The Rio Grande and its tributaries subsequently cut deeply into basin-fill sediments in the rift and, in some places, into the underlying bedrock.

METHODS FOR DETERMINING AGES OF FAULTING

Two methods are used in this study to determine the ages of fault movement. The first method is a stratigraphic approach by which the ages of faulted and unfaulted deposits bracket the age of the most recent fault movement. Recurring episodes of movement often are recognized by comparing the cumulative amounts of displacement in deposits of different ages. **A** second method is to infer ages of undated fault scarps through a quantitative comparison of their morphology with morphologies of dated scarps. This latter method is discussed in the section entitled Scarp Morphology Methods.

Stratigraphic Methods

The distributions of young basin-fill deposits and volcanic rocks, surficial deposits, and some of the faults shown in Figure I are from maps by Lambert (1966), Kelley (1977), Manley and others (1978), and Lipman and Mehnert (1979), and from examination of aerial photographs. Pliocene and younger deposits were divided into four categories to provide age controls of fault movement. The oldest category, of Pliocene to early Pleistocene age (5.0-0.75 m.y.), mainly includes flows of the Servilleta Basalt, as well as local rhyolitic to rhyodacitic rocks and interbedded sediment. This age category also includes late Pliocene to early(?) Pleistocene aluvial-fan and piedmont-slope basin-fill deposits that immediately overlie basalt flows of the upper part of the Servilleta Basalt. The middle and late Pleistocene categories (750,000-150,000 and 150,000-10,000 yrs ago, respectively) include terrace, piedmont-slope, and alluvial-fan deposits graded to drainages that were incised into volcanic rocks of the Taos Plateau and into Miocene and older rocks in the Chama Basin west of the Taos Plateau. The youngest category includes Holocene (<10,000 yrs) alluvium of the lowest terraces, floodplains, and alluvial fans, and also a thin blanket of eolian sand on the southern Taos Plateau (Kelley, 1977).

Scarp-morphology Methods

Studies of slope-degradation processes and the morphology of young fault scarps by Wallace (1977) and recent demonstration of an empirical relation between the height of a fault scarp (14) and its maximum slope angle (0) by Bucknam and Anderson (1979) have established one basis for determining the relative age of a fault scarp. We use this empirical relation to estimate the recency of fault movement for some Quaternary faults in the Taos Plateau region (see Machette, 1982, or Machette and McGimsey, 1983, for more detailed information about this dating method).

Our scarp nomenclature (Fig. 2) is modified from that of Bucknam and Anderson (1979). Measurements of scarp morphology are from detailed topographic surveys made along traverses perpendicular to the

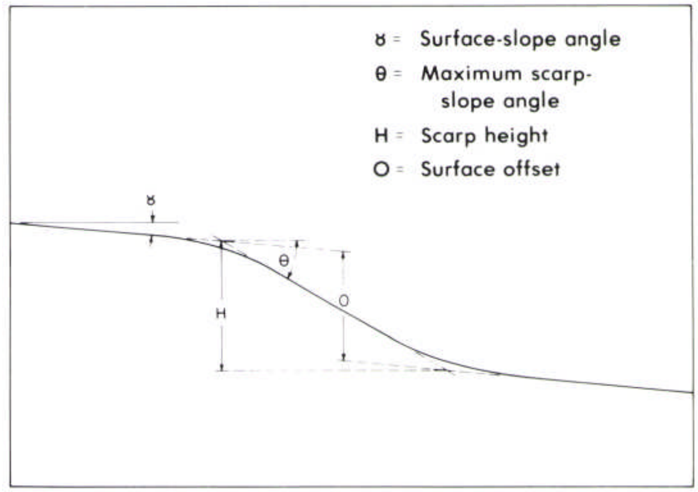

FIGURE 2. Diagrammatic profile of a hypothetical fault scarp (modified from Bucknam and Anderson, 1979, fig. 1).

surface traces of faults. Each traverse yields a scarp profile (Fig. 2), from which measurements of H and 0 (a data pair) were determined. Buchnam and Anderson (1979) showed that a significant correlation exists between the height (1-1) and the maximum slope angle (0) of scarps formed by a single rupture event; a plot of data from a hypothetical scarp profile is illustrated in Figure 3. Data pairs are plotted as open circles and, where there are at least four data pairs, the equation for the line of best fit and the coefficient of determination (r^2) are included.

We used the methods and results of Bucknam and Anderson (1979) and Machette (1982) to assign relative ages to fault scarps. The lines of best fit for two sets of scarp data were used for comparison in Figure 3 and in similar plots of scarp-morphology data (Figs. 6-10). The uppermost dashed line (labeled 5K in Fig. 3) represents combined data from two fault scarps in New Mexico: a fault near the Cox Ranch, just west of White Sands (most recent movement about 4,000 yrs ago; Gile and Machette *in* Seager, 1981; Machette, unpubl. data 1982) and segment C of the La Jencia fault near Magdalena (most recent movement about 5,000 yrs ago; Machette, 1982). The lowermost dashed line (labeled 15K in Fig. 3) is based on R. C. Bucknam's data (written

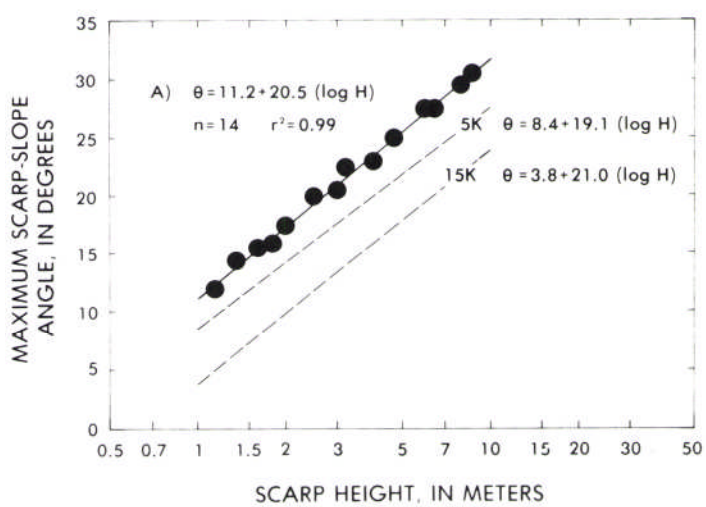

FIGURE 3. Plot of maximum scarp-slope angle (θ) against scarp height (H) for a hypothetical fault scarp. Also shown are the number of data pairs (n), the coefficient of determination (r^2), two reference lines (see text for sources) for age comparisons—5K (4,000–5,000 yrs ago) and 15K (15,000 yrs ago)—and equations for their lines of best fit.

comm. 1980) from the highest wave-cut shoreline of Lake Bonneville, in Utah, which is about 15,000 yrs old based on stratigraphic studies by Scott and others (1984). Although the Bonneville shoreline escarpment is an erosional feature, Bucknam and Anderson (1979) believe it is eroded in the same manner as a fault scarp. Factors (in addition to age) that affect the morphology of a scarp include the texture of the faulted deposits, scarp orientation, and the climate, biological activity, and topographic relief at the scarp site. Although we tried to choose profile sites that minimized these differences, we expected some variation in morphology between scarps of similar age. Therefore, we use the following criteria to assign relative ages to fault scarps: (1) scarps having data sets above the upper dashed line (5K) are considered to be Holocene in age (<10,000 yrs), (2) data sets that occur between the two dashed lines indicate scarps of Holocene or latest Pleistocene age, and (3) data sets that occur below the lower dashed line (15K) indicate scarps of late Pleistocene age (10,000-150,000 yrs old) or, less likely, of middle Pleistocene age (150,000-750,000 yrs old).

Some fault scarps in the region were formed by multiple episodes of surface rupture, as evidenced either by decreasing scarp heights in progressively younger deposits or by scarps that have discrete facets (that is, compound-slope angles) as recognized by Wallace (1977). These compound fault scarps are degraded fault scarps that have been refaulted one or more times (the older scarp slope is noted by the angle 0' in Fig. 4). We interpreted recency of faulting from many compound scarps by assuming that the steepest portion of the scarp (Hs in Fig. 4) is formed by the most recent faulting episode, and that Hs is a close approximation of the most recent offset. Therefore, plots of Hs versus 0 for a compound scarp and plots of H versus 0 for an adjacent single-event scarp should yield similar results. Compound fault scarps usually have Hs versus 0 values (line A in Fig. 5) that plot to the left of Hm versus 0 values (line B in Fig. 5). It is important to note that a fault scarp having a line of best fit with a low-slope value may indicate multiple episodes of faulting even though its resultant scarp does not exhibit compound slope angles.

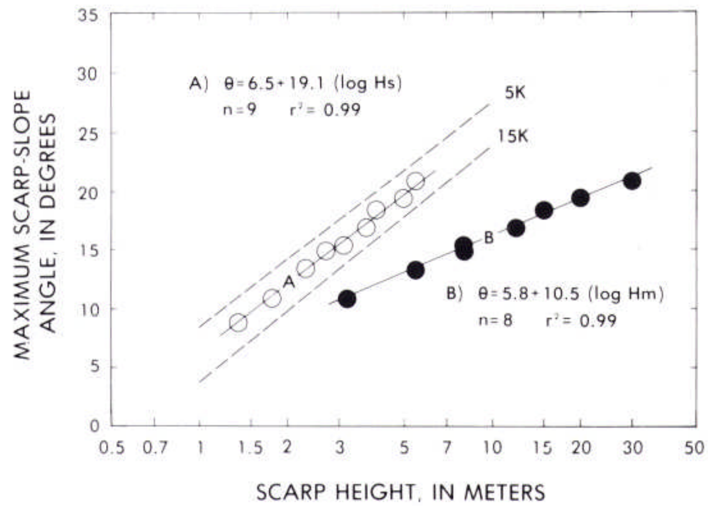

FIGURE 5. Plot of maximum scarp-slope angles (θ) against scarp heights (Hs and Hm) for a hypothetical compound fault scarp. Also shown are the number of data pairs (n), the coefficient of determination (r^2), and two reference lines (see text for sources) for age comparisons—5K (4,000–5,000 yrs ago) and 15K (15,000 yrs ago).

PROMINENT QUATERNARY FAULTS

Most of the following information is based on field investigations conducted during 1980 and 1981, although some data were available from published results of others. The faults are keyed by numbers to Figure 1, and pertinent data for the faults are summarized in Table 1.

Mesita Fault (1)

The Mesita fault, first mapped by Colton (1976), extends from about 5 km north of Mesita cone in southern Colorado to the east flank of Ute Mountain in northern New Mexico. Only the southern 7 km of its 22-km trace are in New Mexico. The Mesita fault (fault 108 *in* Kirkham and Rodgers, 1981) forms a conspicuous west-facing scarp along the east side of the Sky Valley Ranch 7½' quadrangle (Colorado), where it offsets the west flank of the Quaternary Mesita basalt cone (Tweto, 1979) about 13 m (Kirkham and Rodgers, 1981, p. 25). According to Burroughs (1978), flows of the Pliocene Servilleta Basalt are offset only 15-30 m by the Mesita fault. If so, then much of the fault's post-Servilleta offset is recorded in the 13-m-high scarps on Mesita cone. A strong calcic soil has formed in a 2- to 3-m-thick blanket of eolian sand and reworked basaltic cinders that overlies the basalt. Elsewhere on the Taos Plateau such soils are common in early(?) to middle Pleistocene alluvium.

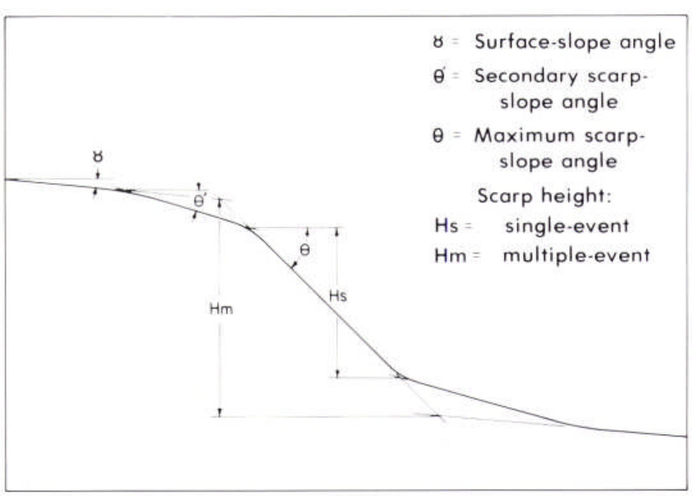

FIGURE 4. Diagrammatic profile of a hypothetical compound fault scarp.

South of Mesita cone, the fault is marked by 5- to 7-m-high south-trending scarps in early(?) to middle Pleistocene alluvium, and in New Mexico by 2- to 5-m-high fault scarps in middle to late(?) Pleistocene alluvium. The later scarps are discontinuous, moderately eroded, and dissected by streams; their gross morphology suggests they are late Pleistocene, but not latest Pleistocene (25,000-10,000 yrs) in age.

Sunshine Valley Faults (2)

Colton (1976) mapped a series of north-trending faults, here collectively named the Sunshine Valley faults, that extends from Sunshine Valley north between Guadaloupe and Ute Mountains. The longest of these suspected faults extends northward 22 km, from a south fork of Latir Creek to a point 6 km due east of Ute Mountain. Although Colton regarded these faults as the southern extension of the Mesita fault (1), we consider them to be separate because they are not continuous with the Mesita fault and have the opposite sense of movement, down to the east.

The Sunshine Valley faults cross an area underlain by late Pleistocene alluvium; however, 1-2 km west (downslope) of the main fault, elongate ridges of middle(?) Pleistocene alluvium occur 5-10 m above stream level. These ridges may be the result of offset along the Sunshine Valley faults and subsequent stream erosion through the uplifted, western block. The longest and easternmost of the Sunshine Valley faults is the only one that coincides with an obvious alignment of vegetation. Although we did not observe a topographic escarpment along this lineament, fine-grained sediment ponded on the east side of the lineament suggests that it coincides with a small fault scarp that now is largely buried. If the Sunshine Valley faults actually cut alluvium, their offsets must be small (less than 5 m). The three suspected faults that Colton (1976) mapped south of Sunshine and west of the main fault were not located in the field.

TABLE 1. Location, recency of movement, and size of some major faults in the Taos Plateau region. Ages: **h,** Holocene; **lp,** late Pleistocene; **mp,** middle Pleistocene; **ep,** early Pleistocene to Pliocene. Symbol **e** indicates scarp height estimated from 7½′ topographic map or aerial photograph. Types of fault movement are determined from scarp morphology, age determination of faulted deposits, and/or map pattern; all faults are normal except as noted.

Map No.	Fault name(s)	Location	Age of most recent movement	Measured scarp heights (m)	Age of displaced deposits	Fault length (km)	Type of fault movement	References
1	Mesita	E of Ute Mountain	lp	2-5e	ep-lp	22	Recurrent	Colton, 1976; Burroughs, 1978; Kirkham and Rodgers, 1981
2	Sunshine Valley (new name)	E of Sunshine, 14 km SSW of Costilla	lp?	<5e	mp?-lp	2-13	Unknown	Colton, 1976
3	Cedros Canyon (new name)	5-12 km S of Costilla E of NM Hwy 85	lp	2-14	mp-lp	7	Recurrent	Upson, 1939
4	Urraca Ranch (new name)	12 km S of Costilla at Urraca Ranch	lp	17	mp-lp?	2	Recurrent	Upson, 1939
5	Taos Pueblo (new name)							
	North part	2 km NE of Taos Pueblo	lp	2-18	ep-lp	5	Recurrent, segmented	None
	South part	2 km E of Taos, N to Rio Pueblo de Taos	lp	2-7	mp?-lp	5		None
6	Canon (new name)	E of Taos, from Canon S to Talpa	lp-h?	2-5	ep?-lp	6	Recurrent	Lambert, 1966, p. 47
7	Los Cordovas (new name)	N of Los Cordovas, 10 km W of Taos	ep-mp?	<15-30e	ep-mp?	<8-12	Unknown, many faults	Lambert, 1966, p. 47
8	Embudo (Picuris frontal fault)	Hondo Canyon, SW along Rio Grande, coincident with Jemez lineament	lp?	7-15	ep-mp	>32 to 75	Recurrent, reverse to normal	Lambert, 1966, p. 47; Muehlberger, 1979, p. 77-82

Sangre de Cristo Fault Zone (Faults 3-6)

The Sangre de Cristo fault zone is one of the major Pliocene and Pleistocene structures of the Taos Plateau. The fault zone bounds the west side of the Sangre de Cristo Mountains along most of their 160-km length in southern Colorado and northern New Mexico. Scott (1970) first mapped many of the faults in this zone, and more recently Kirkham and Rodgers (1981) and McCalpin (1983) demonstrated that Holocene or late Pleistocene movement occurred along most of the Sangre de Cristo fault zone in Colorado. Information about the fault zone in New Mexico is limited mainly to our sparse scarp-morphology data from faults in the Costilla (Cedro Canyon fault, 3; Urraca Ranch fault, 4) and Taos areas (Taos Pueblo fault, 5; Cation fault, 6). Our data suggest that the New Mexico portion of the Sangre de Cristo fault zone was less active in the late Quaternary than the portion of the fault zone in Colorado.

The Sangre de Cristo fault zone extends northward from New Mexico into southernmost Colorado along the west side of the San Pedro Mesa. Kirkham and Rodgers (1981) referred to this segment as the West San Pedro Mesa fault. San Pedro Mesa is capped by flows of 3- to 4-m.y.-old Servilleta Basalt that overlie poorly consolidated sediment of the Santa Fe Group; as a result, the West San Pedro fault is covered by landslide debris along most of its length. Burroughs (1978) estimated that basalts west of the fault at the base of San Pedro Mesa have been displaced at least 600 m; this offset corresponds to an average rate of uplift of 150-200 m/m.y. since the basalts were deposited. Immediately southeast of Costilla, the southernmost remnant of the basalt of San Pedro Mesa is uplifted 240-360 m above the adjacent plain of the Taos Plateau. Here the minimum average rate of uplift is 60-120 mim.y.

Cedro Canyon Fault (3)

The surface trace of the Cedro Canyon fault extends from a point 5 km south of Costilla, New Mexico, south and south—southwest about 7 km. This fault is a westward splay of the main range-bounding fault, which is poorly expressed in this area. The fault is named for Cedro Canyon, the source area of a series of alluvial-fan deposits that are offset by the fault. Upson (1939, p. 731) first mapped the fault and showed its scarp in a photograph taken from a point 6.7 km south of Costilla. Here the fault forms a conspicuous 4- to 14-m-high scarp just east of New Mexico State Highway 3.

The Cedro Canyon fault offsets locally derived alluvial-fan debris of middle to late(?) Pleistocene and possibly early Pleistocene age. However, the latest Pleistocene to Holocene alluvial-fan sediments of Cedro Canyon bury the fault scarp at its north end. Although Upson (1939) considered the fault to be Holocene, stratigraphic evidence suggests that the most recent fault movement predated the Holocene; however, the scarp data suggest it need not be older than latest Pleistocene.

The Cedro Canyon fault scarps record multiple episodes of surface offset. The larger scarps are about 8-9 m high in old alluvium and have compound scarp-slope angles indicating young movement superposed on older, degraded scarps. South of the road to Urraca Ranch, single-event scarps less than 4 m high are in younger late(?) Pleistocene alluvium. Figure 6 shows the relation between both single (Hs)- and multiple-event (Hm) scarp heights and maximum scarp-slope angles (0)

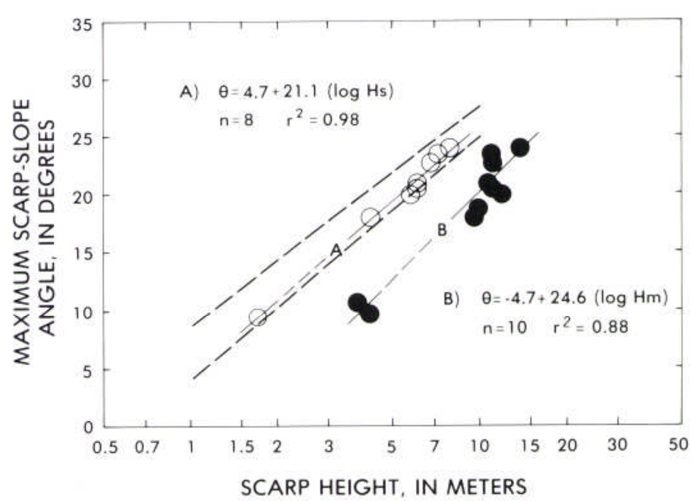

FIGURE 6. Plot of maximum scarp-slope angles (θ) against scarp heights (Hs and Hm) for the Cedro Canyon fault (3). Open circles (line A) are for most recent single-event part of scarp; filled circles (line B) are for entire multiple-event scarp.

for the Cedro Canyon fault. These data also suggest that the latest Pleistocene (10,000-25,00 yrs ago) movement produced scarps 2-8 m high (Hs values).

Urraca Ranch Fault (4)

Upson (1939, p. 731) mentioned a second fault in the Costilla area, here named the Urraca Ranch fault. This fault occurs at the mountain front and forms a prominent scarp across an alluvial fan at the mouth of Jaroso Canyon (La Jara Creek of Upson). The scarp is preserved a short distance adjacent to Jaroso Canyon; it is eroded or poorly developed farther to the north and south along the mountain front.

The soil in the fan alluvium is either early late Pleistocene or late middle Pleistocene in age, judging from the presence of a 0.5- to 1m-thick, reddish-brown, clay-enriched (argillic) B horizon in the upper part of the alluvium. Upson (1939) reported a 70-ft (21-m)-high scarp, but the scam we measured at Urraca Ranch is 16.5 m high (Hm) and has a maximum slope angle (0) of 16-17°. These data indicate that this scam is more degraded than similar scams along the Cedro Canyon fault (Fig. 6). Although the scam lacks a compound profile, its large height suggests several episodes of movement since the middle Pleistocene; the most recent movement may have occurred during late Pleistocene time, because the scam still has a relatively steep slope.

Taos Pueblo Fault (5)

The Taos Pueblo fault forms a sinuous escarpment that trends roughly northwest and southwest, north and south of Taos Pueblo, respectively. The fault is separated into two segments by the Rio Pueblo de Taos where it emerges from the mountains. The heights of scams vary from <2 to 18 m along the northern segment and from <2 to 7 m along the southern segment. The fault forms single, double, and compound scams along a curving, concave-westward trace about 10 km long and 0.5-1.5 km basinward of the mountain front.

The northern segment of the fault typically has an 8- to 15-m-high scam that locally splits into two closely spaced scams, each with heights of 5-12 m. Due north of Taos Pueblo the fault trends northwest and cuts early(?) to middle Pleistocene coarse-grained fan alluvium. Farther north the fault parallels the mountain front and displaces late(?) Pleistocene alluvium less than 2 m. Scam data from the northern segment (Fig. 7) show clear evidence of recurrent fault movement, the most recent of which produced 3- to 7-m-high scarps during the late Pleistocene.

The southern segment of the fault forms two nearly parallel southwest-trending scams in middle to late Pleistocene piedmont-slope alluvium. These scams are less than 2-3 m high, but join about 2 km

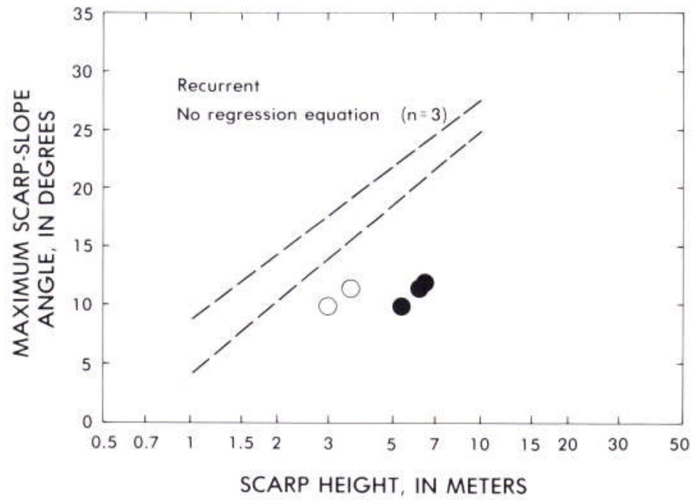

FIGURE 8. Plot of maximum scarp-slope angles (θ) against scarp heights (Hs and Hm) for the southern segment of the Taos Pueblo fault (5). Open circles are for the most recent, single-event part of scarp; filled circles are for the entire multiple-event scarp.

south of Taos Pueblo to form a single scam 5-6 m high (Hm, Fig. 8). The most recent rupture on the combined fault produced scams 3-4 m high (Hs, Fig. 8) during the late Pleistocene, as indicated by the compound nature of the scam. However, this most recent episode of movement may not be as young as that along the northern segment of the Taos Pueblo fault.

Callon Fault (6)

The Canon fault forms small scams east and south of Cation, a small town at the base of the Sangre de Cristo Mountains 1.6 km east—southeast of Taos. We traced these fault scams from a point due east of Canon, where the fault places Pleistocene alluvium in contact with downdropped Pennsylvanian rocks (Lambert, 1966), south and southwest to 1.5 km north of Talpa, a distance of about 6 km. South of the Rio Fernando de Taos the fault cuts late and middle to early(?) Pleistocene piedmont-slope alluvium. The scam-morphology data (Fig. 9) shows multiple-event scam heights (Hm) of 3.5 to 5.4 m and single-event scam heights (Hs) of 1.8-3.4 m. The most recent movement on the Callon fault was either early Holocene or latest Pleistocene in age.

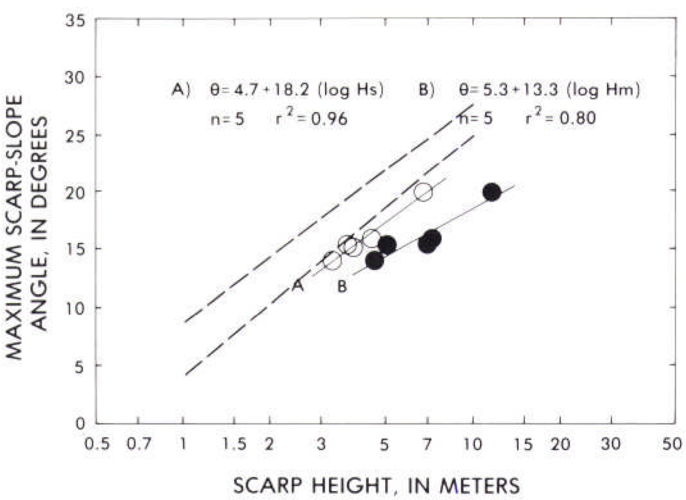

FIGURE 7. Plot of maximum scarp-slope angles (θ) against scarp heights (Hs and Hm) for the northern segment of the Taos Pueblo fault (5). Open circles (line A) are for most recent, single-event part of scarp; filled circles (line B) are for entire multiple-event scarp.

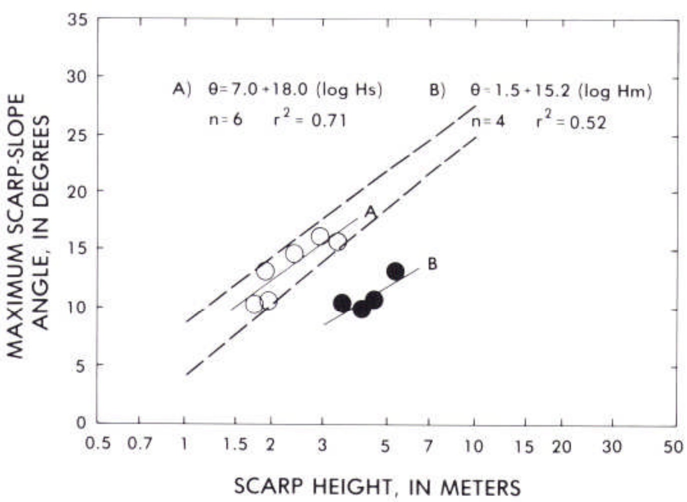

FIGURE 9. Plot of maximum scarp-slope angles (θ) against scarp (Hs and Hm) for the Cañon fault (6). Open circles (line A) are for most recent, single-event part of scarp; filled circles (line B) are for entire multiple-event scarp.

Los Cordovas Faults (7)

Los Cordovas faults are here named for a 5- to 8-km-wide zone of north-trending normal faults that extend about 12 km northward from the Rio Taos near Los Cordovas, New Mexico, to just south of U.S. Highway 64, which crosses the Rio Grande gorge west of Taos (Fig. 1). In areas of greatest offset, the faults place gravelly piedmont-slope alluvium of the uppermost Servilleta Formation (terminology of Lambert, 1966) down-to-the-west against stratigraphically lower 3- to 4-m.y.-old basalt (Lambert, 1966, p. 47). The alluvium probably is no older than late Pliocene or early Pleistocene, but clearly is older than the middle to late Pleistocene terrace alluvium found along major streams in the Taos area. Thus, movement on Los Cordovas faults may be as old as early Pleistocene, or as young as middle(?) Pleistocene.

Erosion of the piedmont gravel has produced west-facing scarps 1530 m high, although the net offset is probably more. Most of the faults are poorly exposed because they are covered by alluvium that fills structurally controlled south-trending valleys.

Lambert (1966, fig. 1) showed only the more prominent Los Cordovas faults. Our photo reconnaissance confirms that most of the drainage in the area between Taos, the Rio Grande gorge, and the Rio Taos is structurally controlled by a combination of these north-trending faults and the southeast-dipping flank of the gorge arch (anticline) as mapped by Muehlberger (1979, fig. 2). Because Los Cordovas faults do not extend very far north of the axis of the gorge arch, the drainage in this area is directed to the west, down the piedmont slope toward the Rio Grande, rather than to the north. Near Los Cordovas, the Rio Taos follows a nearly straight course parallel to the axis of the gorge arch, suggesting that the river may overlie the axis of a previously unmapped syncline. Muehlberger (1979) suggested that the gorge arch (and by association our inferred syncline) resulted from northwestward-directed compression and thrusting of the Picuris Mountains block over the southern Taos Plateau along the Embudo fault (8) during the late Cenozoic.

Embudo Fault (8)

The Embudo fault extends 75 km along a general N 60˚ E trend and connects the northern part of the Espanola Basin with the southern part of the San Luis Basin. The few exposures we have seen along the northeastern part of the Embudo fault show high- to low-angle dip and reverse movement, whereas the movement along its southeastern part is inferred to be normal. The fault changes from normal to reverse sense of movement (the hinge point) near Embudo, where both northward and southward down-dip movement is recorded in the Servilleta Basalt. The southern part of the fault is considered to be the north-bounding structure of the Espanola Basin.

We feel that Muehlberger's detailed maps (1979) of road cuts near Hondo Canyon convincingly demonstrate that the Embudo fault has reverse movement. In the northernmost roadcut (Muehlberger, 1979, roadcut 1 of fig. 4) very coarse Pliocene alluvium of the Servilleta Formation (his terminology) is thrust over middle to early(?) Pleistocene post-Servilleta alluvium and fault-scarp colluvium. The Pleistocene age of the tectonically buried alluvium is inferred from the presence of a well-developed calcic soil having a discontinuous stage-Ill to stage-IV K horizon.

We measured two scarp profiles on the piedmont slope adjacent to and above Muehlberger's roadcut 1 (1979, fig. 3). Northeast of the road cut, the scam has a height of about 15 m, whereas to the southwest it is only 7 m high (Hm, Fig. 10). However, the crest and backslope of the smaller scam has been eroded and its height is therefore a minimum value. The morphology of the fault scarp is similar to that of scarps formed by late Pleistocene normal faults, although we cannot be certain that such comparisons are valid.

Northeast of Hondo Canyon, the Embudo fault splits into several parallel strands that form low, discontinous scams in early to middle(?) Pleistocene sediment. This part of the fault is inferred to continue eastward near the base of the Picuris Mountains and to connect with the Canon fault southeast of Ranchos de Taos.

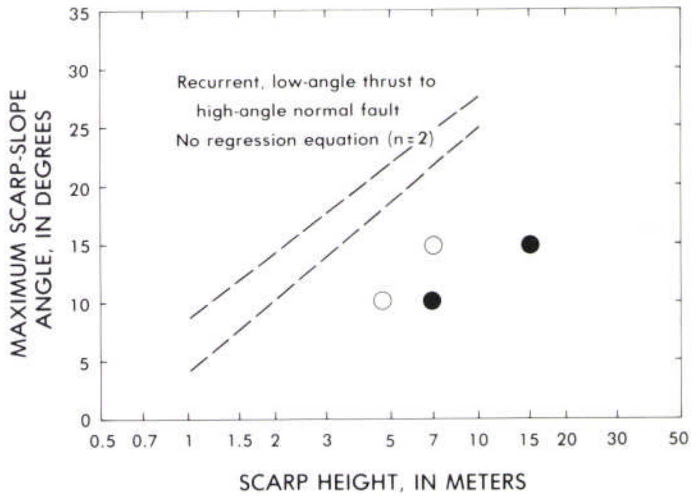

FIGURE 10. Plot of maximum scarp-slope angles (θ) against scarp heights (Hs and Hm) for the Embudo fault (8). Open circles are for the most recent, single-event part of scarp; filled circles are for entire multiple-event scarp.

CONCLUSIONS

Pliocene and Quaternary faults are abundant in the Taos Plateau region of the Rio Grande rift in northern New Mexico. These faults cut early(?) to latest Pleistocene sediments, Pliocene basalts, and Pliocene to early(?) Pleistocene basin-fill deposits. Morphologic, pedologic, and geologic data collected along some of the major fault scarps indicate that many were formed during the late Pleistocene (150,000-10,000 yrs ago), and some as recently as latest Pleistocene (25,000-10,000 yrs ago).

Our morphometric data suggest that significant surface rupturing of early Holocene or latest Pleistocene age may have occurred on the Canon fault (6), which is here considered to be the southernmost segment of the Sangre de Cristo fault zone. Faults with evidence of latest Pleistocene surface rupturing include the Cedro Canyon fault (3) and the northern segment of the Taos Pueblo fault (5). In addition, faults along which the most recent surface ruptures date from the late Pleistocene include the Mesita (I) and Sunshine Valley (2) faults, the Urraca Ranch fault (4), the south segment of the Taos Pueblo fault (5), and possibly the Embudo fault (8). The Los Cordovas faults (7) are known only to be younger than the Pliocene to early(?) Pleistocene deposits which they displace; however, we suspect they may have experienced middle Pleistocene movement.

Fault scarps formed in middle to late Pleistocene surficial deposits in the region are as much as 18 m high; faults with recurrent movement generally have scarps higher than 7 m. The largest scarps are in Pliocene to early Pleistocene deposits along the Los Cordovas (7) and the Embudo (8) faults and early to middle Pleistocene alluvium along the Cedro Canyon fault (3); these scarps clearly are the product of recurrent movement, as evidenced by decreasing amounts of displacement in progressively younger deposits.

The Sangre de Cristo fault zone and the Embudo fault form the eastern and southeastern boundaries, respectively, of the Pliocene- to Pleistocene-age Rio Grande rift on the southern Taos Plateau. Farther south in the Espanola Basin, the Embudo and Pajarito faults (not discussed here) form the north and west margins of the rift, respectively. The Embudo fault lies coincident with the Jemez lineament, across which the rift abruptly changes geometry from the thick, east-dipping strata of the southern San Luis Basin to the thinner, west-dipping strata of the Espanola Basin.

Many faults on the Taos Plateau have displaced Pliocene and Quaternary deposits. In view of the distribution, size, and number of faults that could have histories of recurrent movement in this area, earthquakes and surface ruptures may have been associated with many tens of faults or fault segments during the last 5 m.y. Flows of Servilleta Basalt along the Sangre de Cristo fault zone near the Colorado-New Mexico border have been displaced a minimum of 240-360 m to perhaps as much as 600 m. These data indicate minimum average rates of uplift of 60-120 mim.y. for the past 3-4 m.y.; these rates are comparable to those estimated for other major rift-bounding fault zones in central and southern New Mexico.

REFERENCES

Baldridge, W. S., Bartov, Y., and Kron, A., 1983, Geologic map of the Rio Grande rift and southeastern Colorado Plateau, New Mexico and Arizona; *in* Riecker, R. E. (ed.), Rio Grande rift-tectonics and magmatism: Washington D.C., American Geophysical Union, 2nd printing (1982), scale 1:500,000.

__, Damon, P. E., Shafiqullah, M., and Bridwell, R. J., 1980, Evolution of the central Rio Grande rift, New Mexico-new potassium-argon ages: Earth and Planetary Science Letters, v. 51, pp. 309-321.

Bucknam, R. C., and Anderson, R. E., 1979, Estimation of fault-scarp ages from a scarp-height-slope-angle relationship: Geology, v. 7, pp. 11-14.

Burroughs, R. L., 1978, Northern rift guide 2-Alamosa to Antonito, Colorado; *in* Hawley, J. W. (compiler), Guidebook to the Rio Grande rift in New Mexico and Colorado: New Mexico Bureau of Mines and Mineral Resources, Circular 163, pp. 33-36.

Chapin, C. E., 1979, Evolution of the Rio Grande rift-a summary; *in* Riecker, R. E. (ed.), Rio Grande rift-tectonics and magmatism: Washington, D.C., American Geophysical Union, pp. 1-5.

Colton, R. B., 1976, Map showing landslide deposits and late Tertiary and Quaternary faulting in the Fort Garland-San Luis area, Colorado-New Mexico: U.S. Geological Survey, Open-file Report 76-185, scale 1:250,000.

Cordell, L., 1978, Regional geophysical setting of the Rio Grande rift: Geological Society of America, Bulletin. v. 89, pp. 1073-1090.

Dungan, M. A., Muehlberger, W. R., Leininger, L., and others, 1984, Volcanic and sedimentary stratigraphy of the Rio Grande gorge, and the late Cenozoic geologic evolution of the southern San Luis Valley: New Mexico Geological Society, Guidebook 35 (this volume).

Galusha, T., and Blick, J. C.. 1971, Stratigraphy of the Santa Fe Group, New Mexico: American Museum of Natural History, Bulletin 144, 127 pp.

Hawley, J. W. (compiler), 1978, Guidebook to the Rio Grande rift in New Mexico and Colorado: New Mexico Bureau of Mines and Mineral Resources, Circular 163, 241 pp.

Kelley, V. C., 1977, Geology of the Espanola Basin, New Mexico: New Mexico Bureau of Mines and Mineral Resources, Geologic Map 48, scale 1:125,000.

Kirkham, R. M., and Rodgers, W. P., 1981, Earthquake potential in Colorado - apreliminary evaluation: Colorado Geological Survey, Bulletin 43, 171 pp.

Lambert, P. W.. 1966, Notes on the late Cenozoic geology of the Taos-Questa area, New Mexico: New Mexico Geological Society, Guidebook 17, pp. 43-50.

Lipman, P. W., and Mehnert, H. H., 1979, The Taos Plateau volcanic field, northern Rio Grande rift, New Mexico; *in* Riecker, R. E. (ed.), Rio Grande rift-tectonics and magmatism: Washington, D.C., American Geophysical Union, pp. 289-312.

Machette, M. N., 1982, Quaternary and Pliocene faults in the La Jencia and southern part of the Albuquerque-Belen Basins, New Mexico-evidence of fault history from fault-scarp morphology and Quaternary geology: New Mexico Geological Society, Guidebook 33, pp. 161-169.

__, and McGimsey, R. G., 1983, Map of Quaternary and Pliocene faults in the Socorro and western part of the Fort Sumner 1° x 2° quadrangles, central New Mexico: U.S. Geological Survey, Miscellaneous Field-studies Map MF-l465-A, scale 1:250,000, 12 pp.

Manley, K., 1979, Structure and stratigraphy of the Espanola basin. Rio Grande rift, New Mexico; *in* Riecker, R. E. (ed.), Rio Grande rift-tectonics and magmatism: Washington, D.C., American Geophysical Union, pp. 71-86.

__, Scott, G. R., and Wobus, R. (compilers), 1978, Preliminary geologic map of the Aztec 1° x 2° quadrangle, northwestern New Mexico and southwestern Colorado: U.S. Geological Survey, Open-file Report 78-466, scale 1:250,000.

McCalpin, J., 1983, Quaternary geology and neotectonics of the west flank of the northern Sangre de Cristo Mountains, south-central Colorado: Colorado School of Mines Quarterly, v. 77, no. 3, 97 pp.

Muehlberger, W. R., 1979. The Embudo fault between Pilar and Arroyo Hondo, New Mexico-an active intracontinental transform fault: New Mexico Geological Society, Guidebook 30, pp. 77-82.

Scott, G. R., 1970, Quaternary faulting and potential earthquakes in east-central Colorado: U.S. Geological Survey, Professional Paper 700-C, pp. C I I-C18.

Scott, W. R., McCoy, W. D., Shroba, R. R., and Meyer, R., 1984, Reinterpretation of the exposed record of the last two cycles of Lake Bonneville, western United States: Quaternary Research, v. 20, no. 3, pp. 261-285.

Seager, W. R., 1981, Geology of the Organ Mountains and southern San Andres Mountains, New Mexico: New Mexico Bureau of Mines and Mineral Resources, Memoir 36, 97 pp.

Tweto, 0., 1979, Geologic map of Colorado: U.S. Geological Survey, Special Map, scale 1:500,000.

Upson, J. E., 1939, Physiographic subdivisions of the San Luis Valley, southern Colorado: Journal of Geology, v. 47, pp. 721-736.

Wallace, R. E., 1977, Profiles and ages of young fault scarps, north-central Nevada: Geological Society of America. Bulletin, v. 88, pp. 1267-1281.

Woodward, L. A., Callender, J. F., and Zilinski, R. E., 1975, Tectonic map of the Rio Grande rift, New Mexico: Geological Society of America, Map and Chart Series MC-11, scale 1:1,000,000.